CHEMIJA
2026. Vol. 37. No. 1. P. 43–52

ISSN 0235-7216 eISSN 2424-4538
DOI: https://doi.org/10.6001/chemija.2026.37.1.5

Sustainable corrosion inhibition of carbon steel in 3.5% NaCl using *Moringa oleifera* leaf extract

Benidir Sofiane[1, 2, 3*],

Sobhi Nour El Houda[4, 5]

[1] *Department of Engineering Process, Faculty of Science and Technology, Chadli Bendjedid University, 36000 El-Tarf, Algeria*

[2] *Laboratory of Materials Physicochemistry (LPCM), Faculty of Science and Technology, Chadli Bendjedid University, 36000 El-Tarf, Algeria*

[3] *Laboratory of Electrochemistry and Materials (LEM), Processes Engineering Department, Faculty of Technology, Ferhat Abbas-Setif 1 University, 19000 Setif, Algeria*

[4] *Department of Chemistry, Water and Environment Science and Technology Laboratory, Mohamed Cherif Messaadia University, Souk-Ahras, Algeria*

[5] *Laboratory of Energy and Electrochemistry of Solid (LEES), University Ferhat Abbas Setif 1, Setif, Algeria*

Corrosion is an unavoidable process in metals, but it can be effectively managed through various techniques. One such approach involves the use of environmentally friendly corrosion inhibitors, commonly referred to as green corrosion inhibitors. *Moringa oleifera* (MO) leaves are renowned for their high concentration of antioxidant compounds; however, their applications have primarily been limited to water purification and food ingredients. Addressing this gap, research was conducted to explore the potential of Moringa leaf extract as a green corrosion inhibitor for X70 steel. The study employed varying concentrations of the leaf extract (0.04, 0.08, 0.1 and 0.2 g·L^{-1}) to identify the optimal performance under 3.5% NaCl conditions. The effectiveness of the MO leaf extract in reducing the corrosion rate was evaluated using Tafel polarisation and electrochemical impedance spectroscopy (EIS) tests. The results demonstrated a significant reduction in the corrosion rate, with the highest inhibition efficiency reaching 83% in the NaCl medium. scanning electron microscopy (SEM) analysis further confirmed the formation of a protective layer on the steel surface, consistent with findings from gravimetric and electrochemical studies. These results highlight the potential of Moringa leaf extract as a sustainable and effective corrosion inhibitor.

Keywords: corrosion, *Moringa oleifera*, green corrosion inhibitors, Tafel plots, EIS analysis

INTRODUCTION

Corrosion of metallic materials has long represented a major scientific and industrial challenge owing to its significant economic, environmental and safety implications [1, 2]. Corrosion of metallic materials has long represented a major scientific and industrial challenge owing to its significant economic, environmental and safety implications [3]. In critical infrastructure sectors such as oil and gas, marine transportation and water distribution, corrosion can lead to severe operational failures and substantial maintenance costs.

Despite extensive research, the complete prevention of corrosion remains unfeasible because of its spontaneous thermodynamic nature. Consequently, the focus of modern corrosion science has shifted toward the development of effective mitigation

* Corresponding author. Email: s.benidir@univ-eltarf.dz

strategies aimed at minimising the corrosion rate and associated costs [4–7]. Among these strategies, the use of corrosion inhibitors has gained prominence as one of the most efficient, economical and technically feasible methods for protecting metallic structures. Inhibitors function by adsorbing onto the metal surface, forming a protective barrier that limits the interaction between the substrate and the corrosive medium [6–9].

Traditionally, corrosion inhibitors have been synthesised from organic or inorganic compounds with a high efficiency; however, many synthetic inhibitors are toxic, non-biodegradable and environmentally persistent [4, 7, 8, 10]. These drawbacks have led to increasing environmental and regulatory concerns, prompting a paradigm shift toward the design and utilisation of sustainable, non-toxic and biodegradable corrosion inhibitors. In this context, plant-derived extracts have emerged as a promising class of 'green inhibitors' due to their rich content of phytochemicals such as alkaloids, flavonoids, tannins, terpenoids, and phenolic compounds, which are capable of adsorbing onto metallic surfaces and forming protective complexes [11–15]. The molecular structures of these compounds, often containing heteroatoms (O, N, S) and π-electron systems, facilitate strong interactions with the metal surface, thereby enhancing corrosion resistance.

Among the various natural sources investigated, *Moringa oleifera* (MO), a member of the Moringaceae family, has attracted particular interest due to its diverse biochemical composition and widespread availability in tropical and subtropical regions. The leaves of *Moringa oleifera* are rich in bioactive compounds such as zeatin, quercetin, β-sitosterol, caffeoylquinic acid and kaempferol, as well as phenolic and flavonoid constituents that exhibit strong antioxidant and complexation abilities. These properties suggest that MO leaf extract could act as an effective, eco-friendly corrosion inhibitor by promoting adsorption at the metal/solution interface and forming a stable protective film [16–22].

The present work investigates the corrosion inhibition performance of *Moringa oleifera* leaf extract for X70 carbon steel in a 3.5% NaCl medium, representing conditions relevant to marine and saline pipeline environments. A combination of electrochemical and surface analysis techniques was employed to elucidate the inhibition mechanism. Electrochemical impedance spectroscopy (EIS) and Tafel polarisation were used to evaluate the corrosion behaviour, Fourier-transform infrared spectroscopy (FTIR) was applied to identify the functional groups involved in the inhibition process, and scanning electron microscopy (SEM) was utilised to examine the surface morphology and confirm the formation of the protective layer.

MATERIALS AND METHODS

Materials preparation

The X70 carbon steel sheets used in this study were 1 mm thick. They are mechanically pressed and cut into 1 cm^2 coupons. Those coupons were used in their cut state without additional polishing. They were degreased in ethanol, dried in acetone and stored in moisture-free desiccators before the corrosion studies began. The weight percentage composition of the carbon steel is as follows: C (0.7 max), Mn (1.06 max), Si (0.34 min), P (0.018 max), S (0.17 max), Ni (0.18 max), Nb (0.019 max), Ti (0.023 max) and the remainder Fe.

Gravimetric experiments

The cleaned and dried samples were weighed before being immersed in their respective 3.5% NaCl test solutions. Tests were conducted with varying inhibitor concentrations. Upon completion, the samples were carefully washed in absolute ethanol, reweighed, and the mean values are presented in Table 1.

Electrochemical measurement

The electrochemical assessment was conducted using a PGZ 301 with the VoltaMaster software for electrochemical impedance studies over a frequency range of 100 KHz to 10 mHz, with a signal amplitude perturbation of 10 mV. The polarisation study was carried out considering ± 250 mV vs E_{corr}, systematically monitored at a scanning rate of 0.5 $mV \cdot s^{-1}$, this scan rate was selected based on previous studies which indicate that this rate provides a good balance between measurement accuracy and experimental duration. This rate allows for the precise detection of corrosion processes without causing significant perturbations to the system [23–25]. A platinum counter electrode

and an Ag-AgCl reference electrode (saturated with KCl) were utilised in this study. A 1 cm^2 carbon steel sample served as the working electrode. The experiments were executed in an aerated solution after 1 h of immersion at 303 K. Each assay was performed three times to verify and ensure the reproducibility of the averages obtained, as assessed using Eqs. (1) and (2):

$$IE_{\%} = \frac{I_{corr} - I_{corr}(inh)}{I_{corr}} \times 100, \quad (1)$$

where I_{corr} and i_{corr} (inh) represent the corrosion current densities before and after the addition of the inhibitor, respectively, and

$$IE_{\%} = \frac{R_{ct} - R_s}{R_{ct}} \times 100. \quad (2)$$

In this case, R_{ct} and R_s refer to the charge transfer resistance and the solution resistance with and without an inhibitor, respectively.

Surface characterisation was performed using a JEOL JSM-6510LV microscope, equipped with an INCA Oxford attachment. Metal coupons were analysed after 48 h of corrosion exposure, both in the presence and absence of the optimal inhibitor concentration.

Inhibitor preparation

As illustrated in Fig. 1, the extraction method used was the maceration process. Moringa leaves were dried in the ambient air and then reduced to a powder form. 100 grams of Moringa powder was dissolved in 1 l of ethanol. The reaction mixture was stirred at room temperature for 24 h. After filtration, the rotary evaporator at ±50°C evaporated the extract for 4 h. The solid obtained was recovered, weighed and used as a green corrosion inhibitor.

RESULTS AND DISCUSSION

Fourier transform infrared spectroscopy (FTIR) method

The Fourier transform infrared spectroscopy (FTIR) technique was employed to analyse the infrared transmission spectrum of Moringa leaf powder. The results obtained from the experiment are presented in Fig. 2.

The FTIR data reveals prominent absorption bands at wavenumbers ranging between 3200 and 3400 cm^{-1}, 2929, 1600, 1450, 1245 and 895 cm^{-1}. The broad band observed between 3200 and 3400 cm^{-1} corresponds to the O–H stretching frequency, indicative of alcohol or phenol groups in a polymer structure. The peak at 2929 cm^{-1} is attributed to the C–H stretching frequency, characteristic of alkanes. The bands at 1450 and 1600 cm^{-1} signify the presence of C=C or =C–H stretching vibrations, suggesting the existence of aromatic rings, typically with four or five rings. The peak at 1245 cm^{-1} represents the C–O stretching vibration, while the band at 895 cm^{-1} corresponds to disubstituted aromatic C–H groups [26]. These are indicative of the presence of polyphenols, flavonoids, alcohols, and carboxylic acids classes of compounds known for their corrosion inhibiting properties due to their ability to adsorb on metal surfaces through electron donation and intermolecular interactions.

Gravimetric measurements

Gravimetric experiments were carried out in the presence and absence of different concentrations of

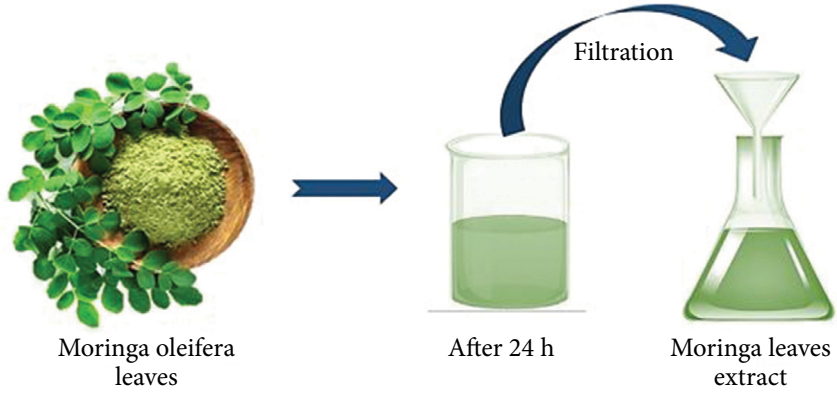

Fig. 1. Extraction process

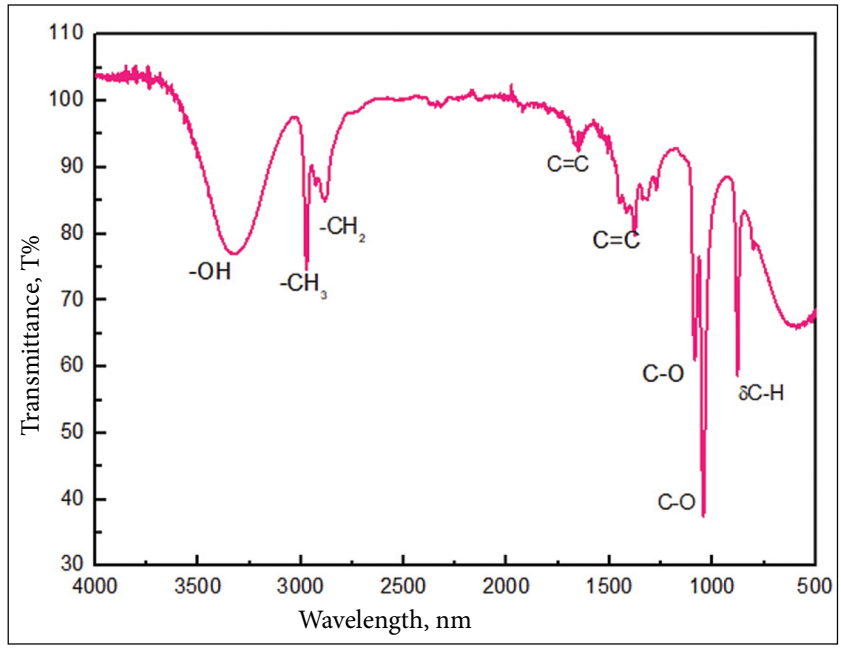

Fig. 2. FTIR spectra of MO

the inhibitor. This technique allows a practical assessment of corrosion conditions, as the inhibitor has a mutual correlation with the liquid phase (it dissolves in water). These exceptional characteristics make this technique more effective for assessing corrosion rates. Table 1 clearly demonstrates that inhibition efficiency increases with higher concentrations of the inhibitor.

Table 1. **The evolution of inhibition efficiency as a function of concentration**

Medium/Concentration, g·L^{-1}	V_{corr}, mm.h^{-1}	*IE*, %	θ
NaCl 3.5%	0.0141	–	–
0.04 g·L^{-1}	0.0037	73.76	0.7376
0.08 g·L^{-1}	0.0029	79.43	0.7943
0.1 g·L^{-1}	0.0023	83.69	0.8369
0.2 g·L^{-1}	0.0025	82.27	0.8227

This phenomenon is typically attributed to the attachment of inhibitor molecules on the degrading metal surface. In the protected medium, particularly at the optimal inhibitor dose, the rate of MO was significantly slower and more inhibited compared to the unprotected medium. This is attributed to the attachment of extract molecules covering the surface fraction of carbon steel [26].

Polarisation curves

Figure 3 signifies the polarisation spectrum of carbon steel (X70) in 3.5% NaCl solution in an unprotected and protected solution.

The addition of *Moringa oleifera* to a 3.5% NaCl solution shifts both the anodic and cathodic axes toward lower dissolution current densities, with this effect becoming more pronounced as the concentration/thickness of *Moringa* molecules increases [27]. Table 2 summarises the electochemicals parameters obtained from the extrapolation Tafel curves.

The parameters obtained from the polarisation study, as depicted in Fig. 3, are summarised in Table 2. Notably, in the 3.5% NaCl solution, the corrosion current density (I_{corr}) is significantly reduced in the presence of *Moringa oleifera* compared to the unprotected medium, and the protection efficiency improves with higher concentrations of *Moringa* molecules. The variations in the cathodic (β_c) and anodic (β_a) Tafel slopes in both environments consistently decrease upon the introduction of *Moringa* molecules, suggesting an effective adsorption mechanism [28].

The inhibition trend observed in Table 2 can be attributed to the adsorption of active phytochemical constituents present in the *Moringa oleifera* extract, such as polyphenols, flavonoids, and organic acids, onto the carbon steel surface. These molecules contain electron-rich functional groups (e.g.

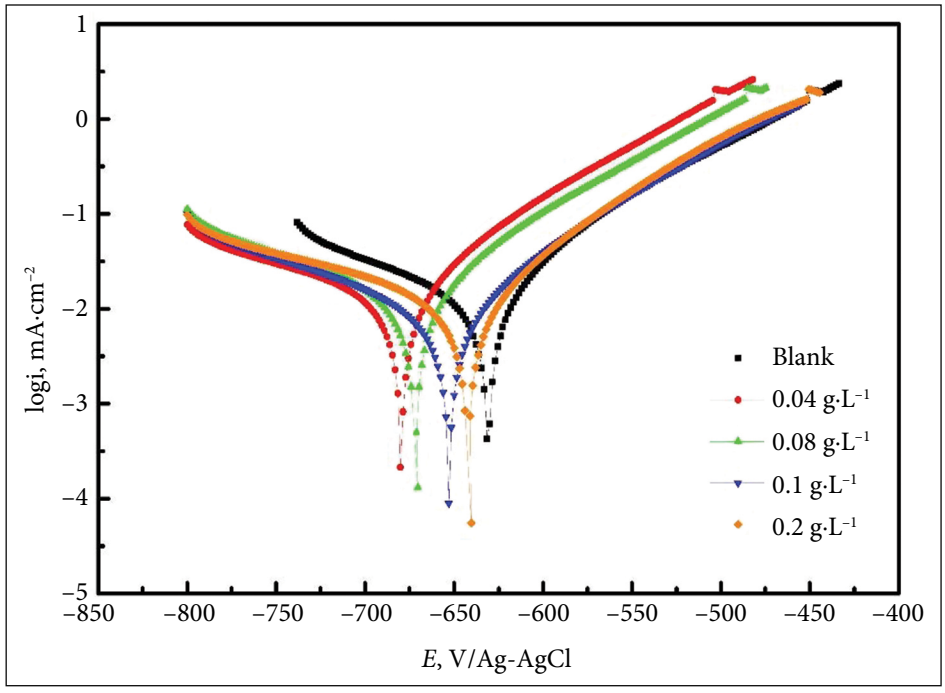

Fig. 3. Polarisation curves for X70 in a sodium chloride solution with and without an inhibitor

OH, C=O, C=C) that can coordinate with vacant d-orbitals of iron atoms, forming a protective barrier that reduces both anodic and cathodic reactions. An inhibitor is typically classified as anodic or cathodic if the shift in the corrosion potential (E_{corr}) upon its addition is less than 85 mV compared to the unprotected solution. In this study, the E_{corr} shift was less than 85 mV, confirming that *Moringa oleifera* functions as a mixed-type inhibitor for the corrosion of X70 steel in a 3.5% NaCl solution, with a predominant cathodic influence [29, 30]. The high inhibition efficiency achieved in the 3.5% NaCl medium underscores the strong activity of *MO* on the carbon steel surface.

Electrochemical impedance (EIS)

Electrochemical impedance spectroscopy (EIS) was employed to investigate the corrosion inhibition performance of the *Moringa oleifera* extract for X70 steel in a 3.5% NaCl solution. The corresponding Nyquist data and the parameters obtained from fitting the results to an appropriate equivalent circuit model are presented in Figs 4, 5 and Table 3, respectively.

The analysis reveals a strong correlation between the inhibitor concentration and corrosion protection. The most direct evidence is the substantial increase in the charge transfer resistance (R_p) upon the addition of the Moringa inhibitor. In the uninhibited solution, the R_p value was recorded at 279.44 Ω cm^2. This value increased dramatically with increasing the inhibitor concentration, reaching a maximum of 1689 Ω cm^2 at the optimal concentration of 0.1 g·L^{-1}. This increase in R_p provides a significant impediment to the charge transfer process that governs the corrosion reaction,

Table 2. **Polarisation curves data for X70 in sodium chloride solution in the presence and absence of inhibitors**

Medium	E_{corr}, mV	I_{corr}, mA·cm^{-2}	R_p, Ω·cm^2	β_a, mV/dec	$-\beta_c$, mV/dec	*IE*, %
Blank	−639	0.607	120	136.6	82.9	–
0.04 g·L^{-1}	−670	0.128	151	82.6	215.2	78.91
0.08 g·L^{-1}	−661	0.115	169	80.1	184.7	81.05
0.1 g·L^{-1}	−652	0.098	190	79.2	166.3	83.86
0.2 g·L^{-1}	−642	0.105	237	71.9	146.8	82.70

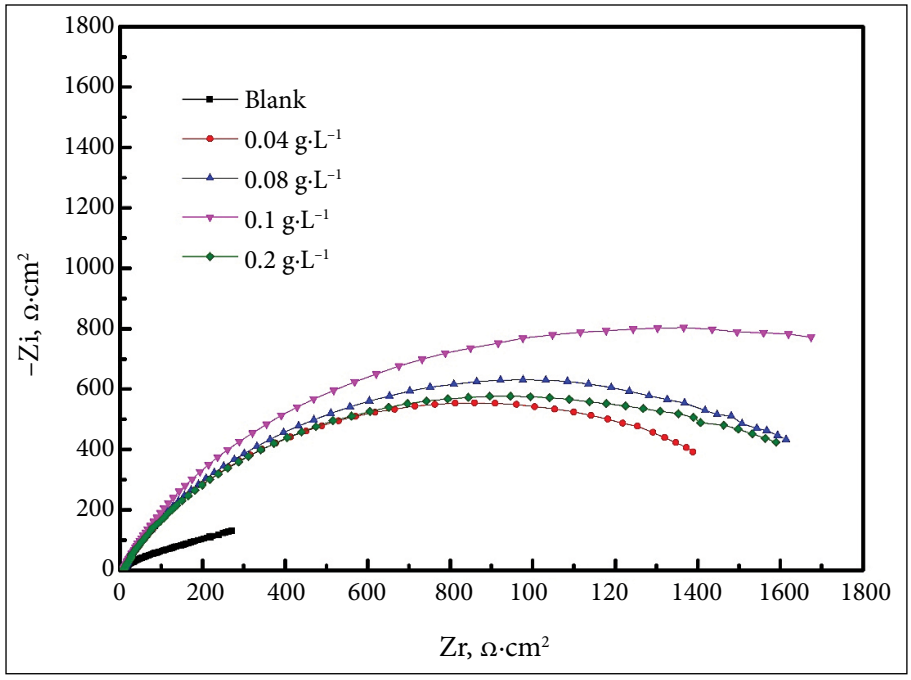

Fig. 4. Electrochemical impedance diagram of X70 steel in 3.5% NaCl without and with different concentrations of a green inhibitor

unequivocally demonstrating the formation of a protective barrier on the metal surface.

The inhibition efficiency (IE%), calculated from the R_p values, further quantifies this performance. The IE% increased with concentration, peaking at 83.46% for the 0.1 g·L^{-1} formulation. A slight decrease in efficiency was observed at the higher concentration of 0.2 g·L^{-1}, which may be attributed to the possible aggregation of inhibitor molecules or saturation/desorption effects at the steel–solution interface [31–35].

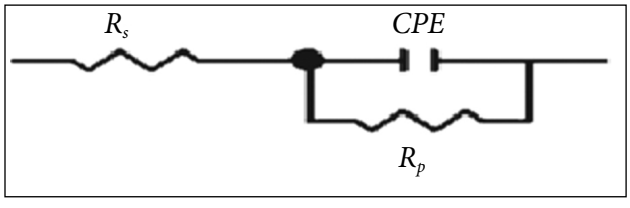

Fig. 5. Model of the equivalent electrical circuit used in the study

Further insight into the inhibition mechanism is provided by the constant phase element (CPE) parameters. A notable decrease in the CPE value was observed with increasing the inhibitor concentration, from 2.482 mF·m^{-2} for the blank to 1.226 mF·m^{-2} at 0.2 g·L^{-1}. This reduction in capacitance is characteristic of the displacement of water molecules (which have a high dielectric constant) from the metal surface by adsorbed inhibitor molecules, which form a protective layer with a lower effective dielectric constant. Concurrently, the n parameter, which reflects the surface homogeneity, increased from 0.59 to approximately 0.75. This shift towards a more ideal capacitive behaviour indicates that the inhibitor film creates a more uniform and smooth surface, effectively passivating the active corrosion sites and leading to a more homogeneous electrode interface.

Table 3. **EIS parameters for X70 in sodium chloride solution in the presence and absence of inhibitors**

C, g·L^{-1}	R_s, Ω·cm²	R_p, Ω·cm²	*CPE*, mF·cm^{-2}	*n*	*IE*, %
0	4.348	279.44	2.482	0.59	/
0.04	3.705	1339	1.845	0.71	79.13
0.08	3.438	1622	1.495	0.74	82.77
0.1	3.198	1689	1.325	0.74	83.46
0.2	2.878	1509	1.226	0.75	81.48

The EIS data confirm that the *Moringa oleifera* extract acts as an effective green corrosion inhibitor for X70 steel in a saline environment. The primary mechanism is via adsorption of its organic constituents onto the steel surface, forming a robust and relatively homogeneous film that blocks the active sites, thereby increasing the charge transfer resistance and reducing the double-layer capacitance. The optimal inhibition efficiency of 83.46% is achieved at a concentration of 0.1 g·L^{-1} [36, 37].

Organic species generally exhibit lower dielectric effects compared to water molecules, so their adsorption leads to the replacement of water molecules on the electrode surface, resulting in a decrease in CPE values [27, 38]. Consequently, the (MO) extract inhibits the corrosion process on X70 steel by facilitating the adsorption of its organic constituents at the metal–solution interface.

SEM analysis

Scanning electron microscopy (SEM) was employed to visually assess the surface morphology of X70 steel specimens after 24 h of immersion in a 3.5 wt.% NaCl solution, both in the absence and presence of the *Moringa oleifera* (MO) extract inhibitor at its optimal concentration of 0.1 g·L^{-1}. The resulting micrographs are presented in Fig. 6.

The micrograph of the specimen immersed in the uninhibited solution (Fig. 6a) reveals a severely damaged surface. The morphology is characterised by a rough and porous topography, with an evident grain attack and the formation of a non-uniform corrosion product layer. This extensive damage is typical of uniform corrosion in an aggressive chloride-containing environment and confirms the corrosive nature of the medium towards X70 steel [39].

In a stark contrast, the micrograph of the specimen exposed to the solution containing 0.1 g·L^{-1} of MO extract (Fig. 6b) exhibits a fundamentally different and significantly improved morphology. The surface is covered by a continuous, coherent and film-like layer. This layer appears smooth and dense, effectively obscuring the underlying microstructure and the original polishing marks.

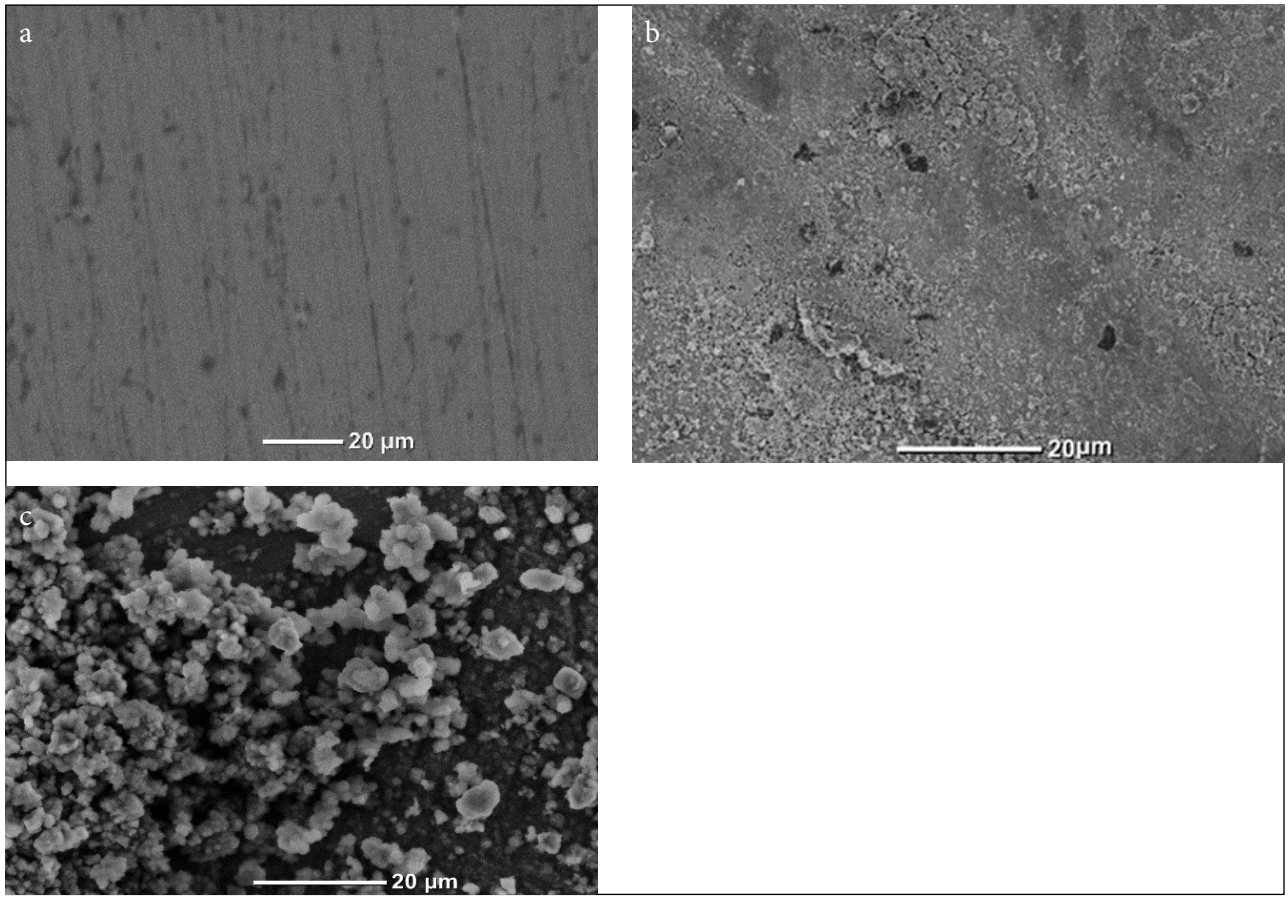

Fig. 6. The SEM images for the carbon steel in NaCl 3.5%; (a) polished sample; (b) in NaCl 3.5%; (c) in NaCl 3.5%+MO 0.1 g·L^{-1}

The absence of the porous corrosion products and the rough features observed in the blank sample is notable.

While this micrograph (Fig. 6c) primarily depicts the protective coating formed *in situ* during immersion rather than the pristine metal substrate beneath it, the presence of this continuous film is a direct physical evidence of the inhibitor's action. The formation of such an adherent layer is consistent with the adsorption of organic constituents from the *Moringa oleifera* extract onto the active sites of the steel surface. This adsorbed film likely functions as a physical barrier, impeding the direct access of chloride ions and water molecules to the metal interface, thereby retarding the corrosion process [40, 41].

This morphological evidence strongly corroborates the electrochemical findings from EIS, which indicated a significant increase in charge transfer resistance and the formation of a more homogeneous surface. The dense and uniform nature of the observed layer aligns well with the increase in the 'n' parameter of the Constant Phase Element, suggesting an improved surface homogeneity due to inhibitor adsorption. Therefore, it is concluded that the high inhibition efficiency of the *Moringa oleifera* extract is achieved through the formation of this protective surface film. To further elucidate the film's thickness, adhesion, and the precise condition of the metal–coating interface, cross-sectional SEM analysis is recommended for future investigations.

Adsorption isotherm

Adsorption isotherms provide a quantitative assessment of the attraction between adsorbate molecules and the surface of the adsorbent. They provide essential information about adsorption capacity, binding strength and the fundamental mechanisms involved in the adsorption process. The surface coverage (θ), calculated from gravimetric data using the equation IE % = (θ × 100), and the concentration of the *Moringa extract* were used to assess the fit of the experimental data to the Langmuir adsorption isotherm [42, 43].

The equation $\frac{c}{\theta}=\left(\frac{1}{K_{ads}}\right)+C$ was applied, where K_{ads} represents the equilibrium constant for the adsorption process of the inhibitor, and C is the inhibitor concentration. The corresponding plot is shown in Fig. 7. The slope of 1.1837 and the high R^2 value of 0.998 indicate that the experimental data closely follow the Langmuir adsorption model. The slight deviation of the slope from unity is often attributed to interactions between adsorbed species on the surface or variations in adsorption energies as surface coverage increases [42, 43].

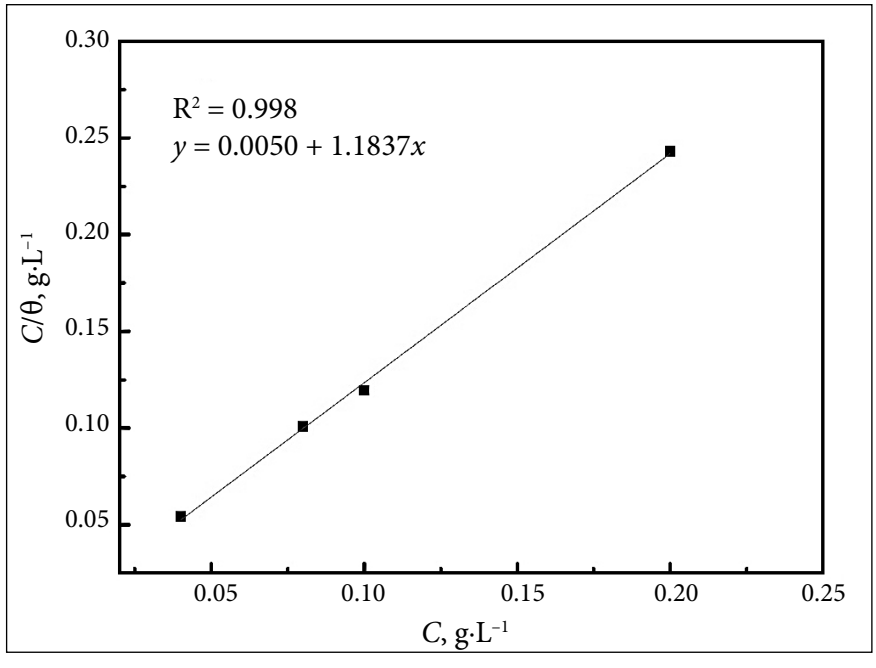

Fig. 7. Langmuir isotherm

The strong alignment of the data with the Langmuir adsorption model further supports the hypothesis that substances contained in *Moringa oleifera* adsorb onto the steel surface. Additionally, the K_{ads} value can be determined from the intercept of the θ/*C* axis on the isotherm plot and is related to the standard free energy of adsorption ($\Delta G°_{ads}$) through Eq. (3),

$$\Delta G°_{ads} = -RT\,Ln\,(1000^{*}K_{ads}), \quad (3)$$

where *R* represents the universal gas constant, *T* is the absolute temperature in Kelvin (K), and the constant value of 1000 g·L^{-1} denotes the concentration of water in the solution. The negative value of $\Delta G°_{ads}$ (–29.349 kJ·mol^{-1}) suggests that the adsorption of substances contained in *Moringa oleifera* on the steel surface is a spontaneous process [38, 44].

It is well documented in the literature that $\Delta G°_{ads}$ values around or below –20 kJ·mol^{-1} typically indicate non-specific or electrostatic interactions between the inhibitor species and the charged metal surface, characteristic of physical adsorption. Conversely, values around or above –40 kJ·mol^{-1} are associated with electron transfer interactions, indicative of chemisorption [45–47]. The adsorption isotherm presented in this study, as shown in Fig. 7, demonstrates that the inhibition mechanism of *Moringa oleifera* leaf extract on X70 steel in a 3.5% sodium chloride solution follows the Langmuir model. This indicates that a monolayer of the extract's active phytochemical constituents is adsorbed onto the steel surface. The adsorbed species mainly include polyphenols, flavonoids, and organic acids, as identified by FTIR analysis in Fig. 2. These compounds contain electron-rich functional groups such as hydroxyl, carbonyl, and carbon–carbon double bonds, which can coordinate with the vacant d-orbitals of iron atoms, thereby forming a protective layer that suppresses both anodic and cathodic corrosion reactions, as demonstrated in the Section 'Polarization curves' and Table 2. The negative value of the standard free energy of adsorption, measured at –29.349 kJ·mol^{-1}, suggests a mixed adsorption mechanism that includes both physical and chemical interactions.

CONCLUSIONS

This study reveals that the Moringa leaf extract exhibits good inhibitory properties. However, further studies are needed to evaluate its long-term stability in harsh environments, including its resistance to oxidation, photodegradation and biodegradation. Overall, it can be concluded that:

1) Moringa leaf powder effectively reduces the corrosion rate of carbon steel in a 3.5% NaCl solution.

2) The corrosion rate and i_{corr} are significantly higher without Moringa leaf powder but decrease as the inhibitor is added.

3) The adsorption mechanism of Moringa leaf powder (MO) follows a mixed behaviour, involving both physical and chemical adsorption.

4) Moringa leaf powder acts as a mixed inhibitor, forming a protective oxide film on the metal surface, which enhances resistance to corrosion.

5) The inhibitor's efficiency increases with concentration, reaching a maximum at 0.1 g·L^{-1}, demonstrating that higher concentrations more effectively block the corrosion process.

6) Surface examination results align with previous studies, confirming the formation of a protective layer on the metal surface.

Received 20 December 2025
Accepted 19 January 2026

References

1. M. Faiz, A. Zahari, K. Awang, H. Hussin, *RSC Adv.*, **10(11)**, 6547 (2020).
2. L. Popoola, A. Grema, G. Latinwo, B. Gutti, A. Balogun, *Int. J. Ind. Chem.*, **4(1)**, 35 (2013) [https://doi.org/10.1186/2228-5547-4-35].
3. S. A. Amadi, C. P. Ukpaka, *Int. J. Appl. Chem. Sci. Res.*, **1(10)**, 182 (2013).
4. M. Oki, A. A. Adediran, P. P. Ikubann, et al., *Results Eng.*, **7**, 100159 (2020).
5. S. A. Akintola, M. Oki, A. A. Aleem, et al., *Results Eng.*, **4**, 100026 (2019).
6. A. S. Adekunle, A. A. Adeleke, P. P. Ikubanni, O. A. Adewuyi, *Nat. Environ. Pollut. Technol.*, **19(3)**, 923 (2020).
7. J. K. Odusote, A. A. Adeleke, P. P. Ikubanni, O. S. Ayanda, J. M. Abdul, R. A. Yahya, *Int. Rev. Appl. Sci. Eng.*, **11(3)**, 269 (2020).
8. A. Singh, E. E. Ebenso, M. A. Quraishi, *Int. J. Corros.*, **2012**, 1 (2012) [https://doi.org/10.1155/2012/897430].

9. O. Olawale, B. T. Ogunsemi, J. O. Bello, P. P. Ikubanni, S. J. Ogundipe, T. S. Abayomi, *Int. J. Mech. Eng. Technol. IJMET*, **9(13)**, 1274 (2018).
10. F. O. Edoziuno, A. A. Adediran, B. U. Odoni, M. Oki, P. P. Ikubanni, O. Omodara, *Sci. World J.*, **2020**, 1 (2020) [https://doi.org/10.1155/2020/2756734].
11. A. Döner, R. Yıldız, S. Arslanhan, M. F. Baran, *J. Taiwan Inst. Chem. Eng.*, **169**, 105955 (2025).
12. R. Solmaz, G. Kardaş, M. Çulha, B. Yazıcı, M. Erbil, *Electrochim. Acta*, **53(20)**, 5941 (2008).
13. S. N. El Houda, B. Amel, F. Malika, *J. Taiwan Inst. Chem. Eng.*, **165**, 105771 (2024).
14. F. Kaya, R. Solmaz, İ. H. Geçibesler, *J. Taiwan Inst. Chem. Eng.*, **143**, 104712 (2023).
15. A. ROMÂNĂ, *Rev. Roum. Chim.*, **68(1–2)**, 17 (2023).
16. M. T. Majd, S. Asaldoust, G. Bahlakeh, B. Ramezanzadeh, M. Ramezanzadeh, *J. Mol. Liq.*, **284**, 658 (2019).
17. M. H. Shahini, M. Ramezanzadeh, G. Bahlakeh, B. Ramezanzadeh, *J. Mol. Liq.*, **332**, 115876 (2021).
18. S. Chen, S. Chen, B. Zhu, C. Huang, W. Li, *J. Mol. Liq.*, **311**, 113312 (2020).
19. C. W. Yaméogo, M. D. Bengaly, A. Savadogo, P. A. Nikiema, S. A. Traore, *Pak. J. Nutr.*, **10(3)**, 264 (2011).
20. J. C. Pereira, L. P. M. Santos, A. A. C. Alcanfor, et al., *Electrochim. Acta*, **407**, 139647 (2022).
21. N. Nweze, *IOSR J. Pharm. Biol. Sci.*, **9(1)**, 99 (2014) [https://www.academia.edu/download/79654996/e47336158b8d83fb3e799cf7bce4b07787be.pdf].
22. R. K. Saini, I. Sivanesan, Y.-S. Keum, *3 Biotech*, **6(2)**, 203 (2016), [https://doi.org/10.1007/s13205-016-0526-3].
23. H. Li, Y. Qiang, W. Zhao, S. Zhang, *Colloids Surf. Physicochem. Eng. Asp.*, **616**, 126077 (2021).
24. S. Boukerche, H. Ferkous, A. Delimi, et al., *Arab. J. Chem.*, **16(9)**, 105061 (2023).
25. A. Berrissoul, E. Loukili, N. Mechbal, et al., *J. Colloid Interface Sci.*, **580**, 740 (2020).
26. S. A. Umoren, U. M. Eduok, M. M. Solomon, A. P. Udoh, *Arab. J. Chem.*, **9**, S209 (2016).
27. E. E. Oguzie, Z. O. Iheabunike, K. L. Oguzie, et al., *J. Dispers. Sci. Technol.*, **34(4)**, 516 (2013),) [https://doi.org/10.1080/01932691.2012.682008].
28. X. Li, S. Deng, H. Fu, *Corros. Sci.*, **62**, 163 (2012).
29. Y. Qiang, S. Zhang, B. Tan, S. Chen, *Corros. Sci.*, **133**, 6 (2018).
30. O. D. Onukwuli, M. Omotioma, *Port. Electrochim. Acta*, **37(2)**, 115 (2019).
31. E. E. Oguzie, C. K. Enenebeaku, C. O. Akalezi, S. C. Okoro, A. A. Ayuk, E. N. Ejike, *J. Colloid Interface Sci.*, **349(1)**, 283 (2010).
32. B. Qian, J. Wang, M. Zheng, B. Hou, *Corros. Sci.*, **75**, 184 (2013).
33. I. M. Mejeha, M. C. Nwandu, K. B. Okeoma, et al., *J. Mater. Sci.*, **47(6)**, 2559 (2012),) [https://doi.org/10.1007/s10853-011-6079-2].
34. X. Wang, H. Yang, F. Wang, *Corros. Sci.*, **55**, 145 (2012).
35. M. Tabyaoui, M. Tourabi, H. Zarrok, et al., *Environ. Sci. Pollut. Res.*, **31(31)**, 43757 (2024),) [https://doi.org/10.1007/s11356-024-34055-6].
36. S. Deng, X. Li, *Corros. Sci.*, **64**, 253262 (2012).
37. F. Kaya, R. Solmaz, İ. H. Geçibesler, *J. Ind. Eng. Chem.*, **122**, 102 (2023).
38. J. Aljourani, K. Raeissi, M. A. Golozar, *Corros. Sci.*, **51(8)**, 1836 (2009).
39. M. G. Fontana, *Corrosion Engineering*, McGraw-Hill, New York (1986) [https://www.osti.gov/biblio/5741236].
40. L. A. Nnanna, I. O. Owate, *Sci. Afr.*, **13(1),** 52 (2014) [https://www.ajol.info/index.php/sa/article/view/157052].
41. F. A. Ugbe, M. A. Funtua, A. V. Ikudayisi, A. A. Pam, *Int. Res. J. Pure Appl. Chem.*, **5(4)**, 331 (2014).
42. E. E. Oguzie, D. I. Njoku, M. A. Chidebere, et al., *Ind. Eng. Chem. Res.*, **53(14)**, 5886 (2014), [https://doi.org/10.1021/ie404273f].
43. E. E. Oguzie, C. B. Adindu, C. K. Enenebeaku, C. E. Ogukwe, M. A. Chidiebere, K. L. Oguzie, *J. Phys. Chem. C*, **116(25)**, 13603 (2012), [https://doi.org/10.1021/jp300791s].
44. E. A. Şahin, Y. A. Dursun, İ. H. Geçibesler, R. Solmaz, *Inorg. Chem. Commun.*, **167**, 112751 (2024).
45. X. Li, S. Deng, H. Fu, *Corros. Sci.*, **53(4)**, 1529 (2011).
46. S. Kherraf, M. Foudia, N. E. H. Sobhi, Z. Djetoui, M. S. Medjram, *Anti-Corros. Methods Mater.*, **72(1)**, 48 (2025).
47. N. E. H. Sobhi, A. Boukhouiete, M. Foudia, S. Benidir, *Rev. Roum. Chim.*, **68(7–8)**, 383 (2023).

Benidir Sofiane, Sobhi Nour El Houda

TVARUS ANGLINIO PLIENO KOROZIJOS SLOPINIMAS 3,5 % NACL TIRPALE NAUDOJANT MORINGOS LAPŲ EKSTRAKTĄ